

# Influence of sectoral structure on Schottky diode and ohmic contact parameters in HPHT diamond

A.S. Nikolenko<sup>1</sup>, V.V. Strelchuk<sup>1</sup>, I.M. Danylenko<sup>1</sup>, D.M. Maziar<sup>1</sup>, Ya.Ya Kudryk<sup>1</sup>,  
T.V. Kovalenko<sup>2</sup>, A.V. Burchenia<sup>2</sup>, V.V. Lysakovskiy<sup>2</sup>, S.O. Ivakhnenko<sup>2</sup>

<sup>1</sup> V.E. Lashkaryov Institute of Semiconductor Physics NASU, pr. Nauky 41, 03028 Kyiv, Ukraine

<sup>2</sup> V. Bakul Institute for Superhard Materials NASU, Avtozavodska str. 2, 04074 Kyiv, Ukraine

## Introduction

Boron-doped diamond (BDD) is increasingly recognized as a premier wide-band-gap semiconductor with exceptional thermal conductivity and a high breakdown field, making it highly relevant for high-power, high-temperature, and radiation-resistant electronic applications. Nonetheless, the formation of a pronounced multi-sector growth structure during high-pressure high-temperature (HPHT) bulk growth poses significant challenges to the operational characteristics of diamond-based devices. Specifically, growth-sector-dependent impurity incorporation kinetics result in severe lateral modulation of uncompensated boron concentration and localized defect density, which can limit the reproducibility of device performance across a single wafer. Utilizing advanced correlative electrical measurements and transmission micro-FTIR ( $\mu$ -FTIR) spatial mapping, we offer a detailed analysis of transport properties in planar Ni/Pt/Au Schottky diodes and Ti/Pt/Au ohmic contacts fabricated on multi-sector HPHT BDD plates. Moreover, we explore the spatial distribution of electrically active boron and its correlation with device leakage statistics, the behavior of discrete shunting defects, and sector-dependent contact resistivity, providing critical insights into optimizing substrate uniformity for high-performance diamond electronics.

## Methods

Multi-sector boron-doped diamond single crystals were synthesized by the temperature gradient method under HPHT conditions in the Fe-Al-C-B system, with {001}, {111}, and {113} growth sectors revealed on the polished (100) substrates. Spatial mapping of the uncompensated boron concentration  $[N_a - N_d]$  across the growth sectors (Fig. 1) was performed via  $\mu$ -FTIR transmission mapping using a Bruker Vertex 70v FTIR spectrometer coupled with a Hyperion 2000 infrared microscope. To study transport properties, arrays of planar Ni/Pt/Au Schottky diodes (100  $\mu$ m diameter) and Ti/Pt/Au ohmic contacts (Fig. 2) were fabricated using photolithography, magnetron sputtering, and rapid thermal annealing at 850°C for 30s. Current-voltage ( $I$ - $V$ ) characteristics of the fabricated structures were systematically measured using a Keithley 2636B SourceMeter under ambient and dark conditions to evaluate rectifying behavior, leakage currents, and specific contact resistivity.

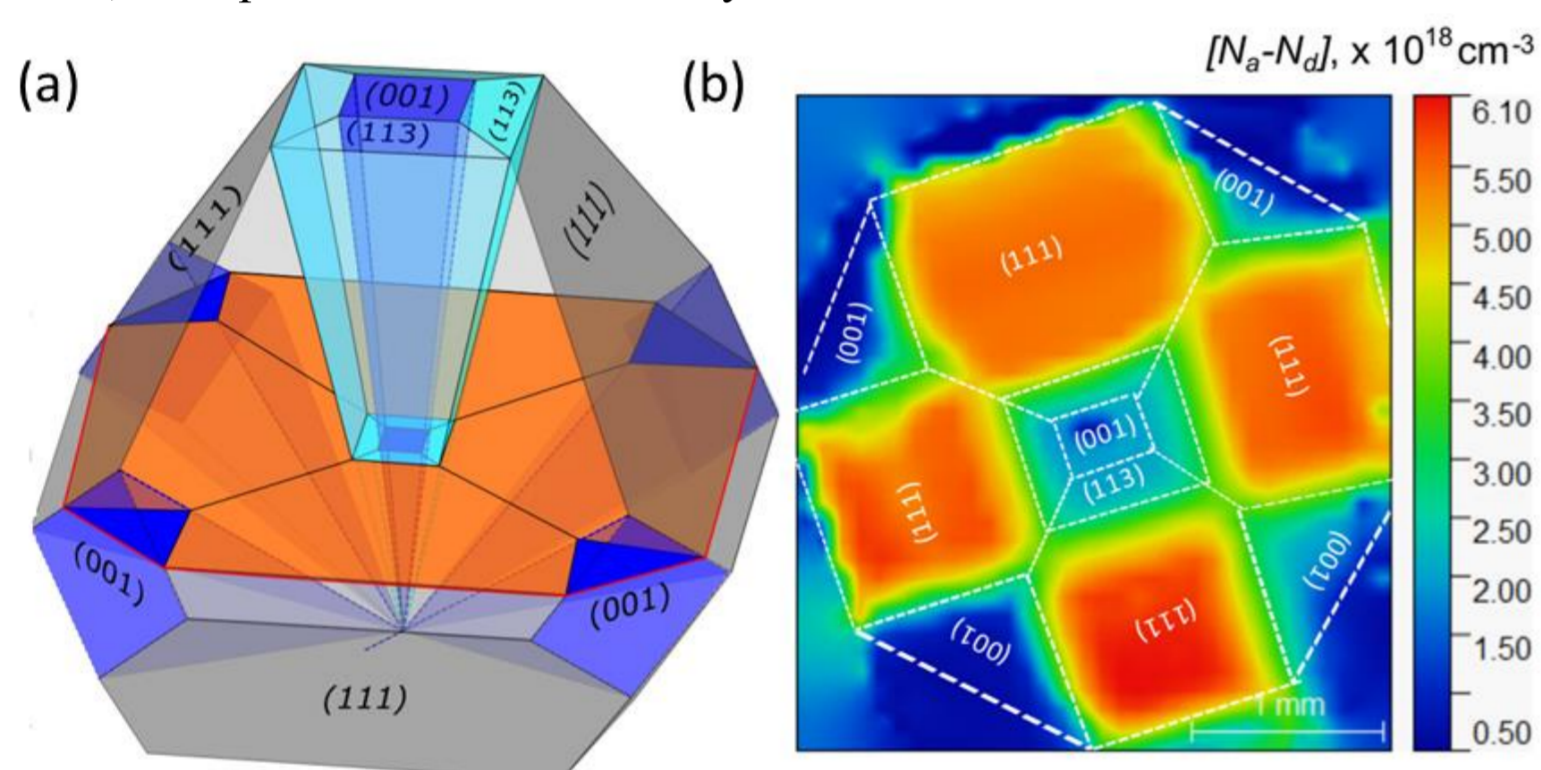


**Fig.1.** (a) Schematic representation of a diamond single crystal indicating the crystallographic growth directions and the cutting plane (red line) of the diamond wafer. (b) Spatial distribution of uncompensated boron concentration across the wafer, obtained by the  $\mu$ -FTIR.

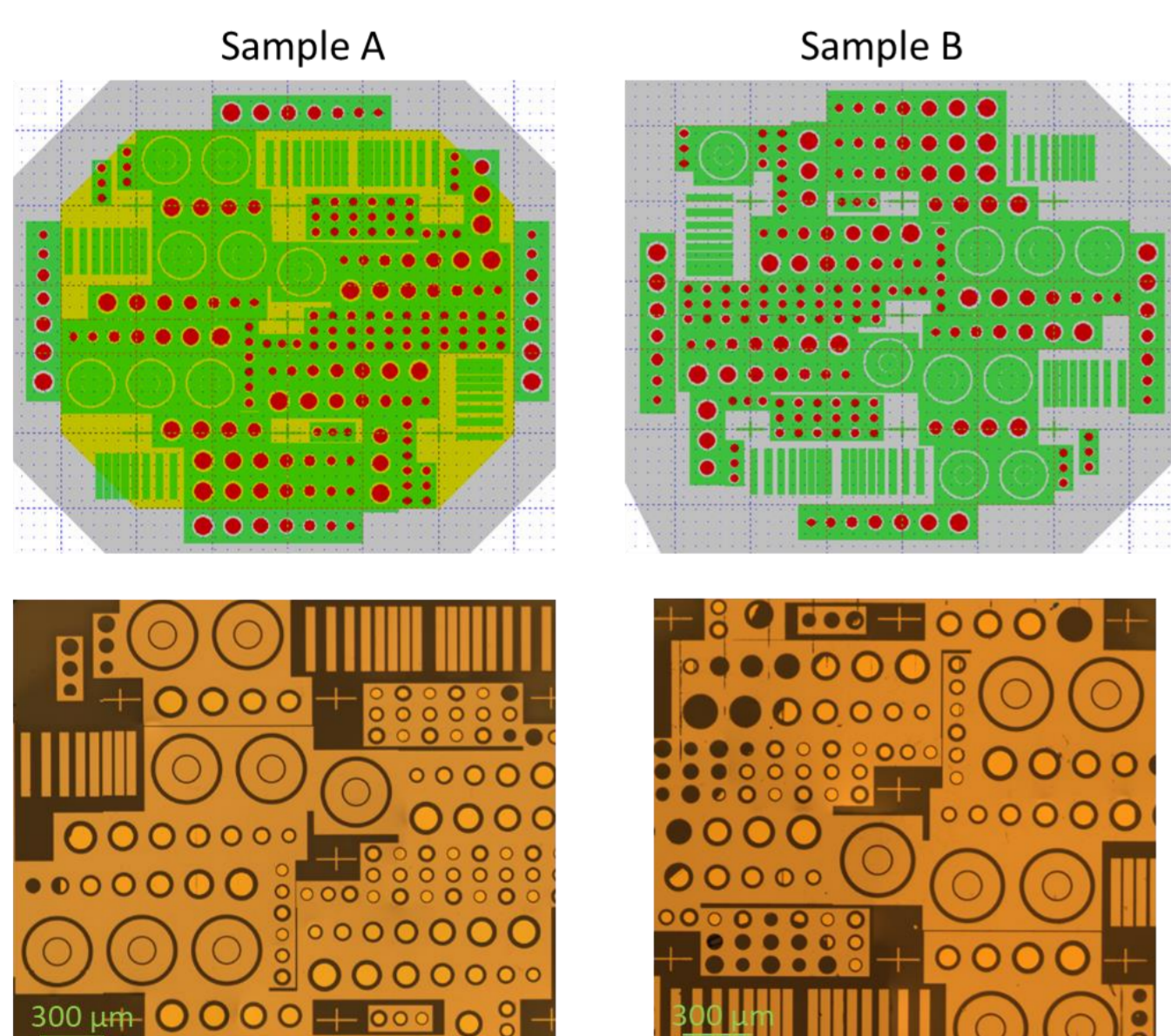


**Fig.2.** Layouts of arrays of Schottky diodes, radial and linear TLM structures with ohmic contacts on multi-sector BDD substrates (top) and the fragment of the as-fabricated structures (bottom).

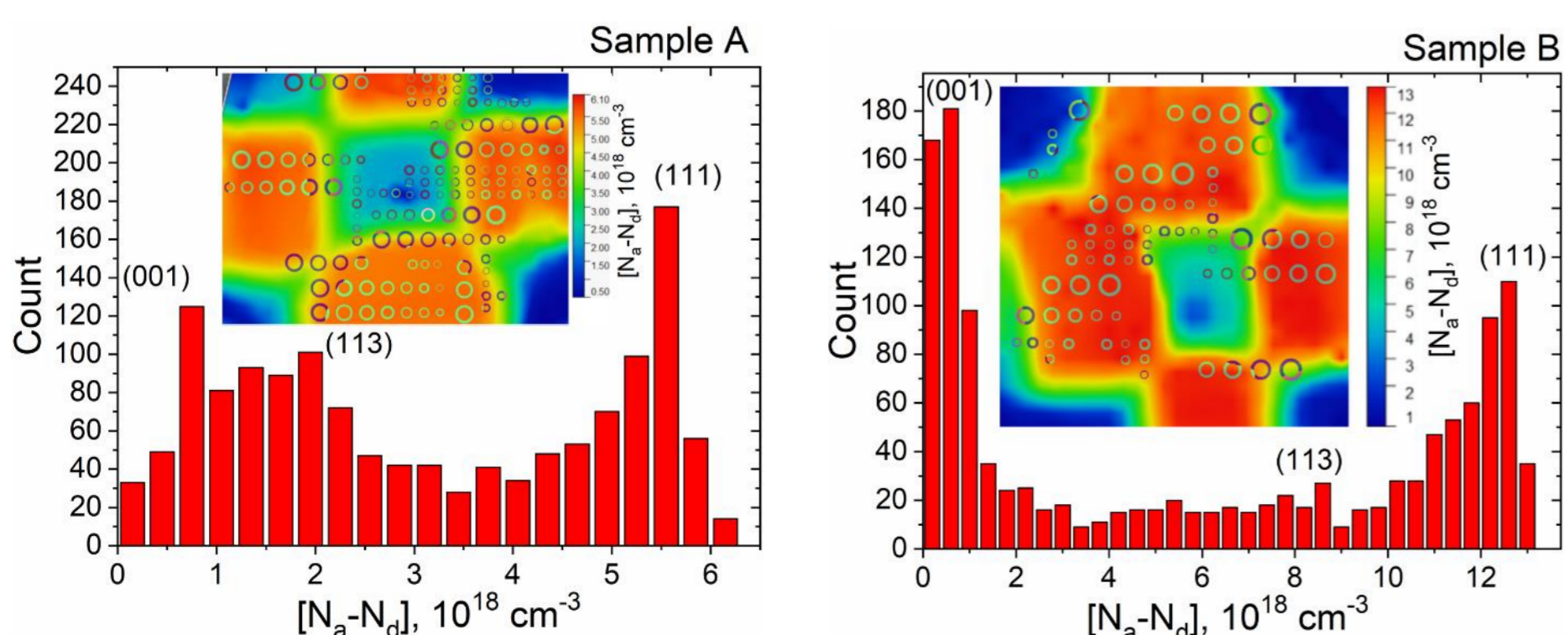


**Fig.3.** Distribution of uncompensated boron concentration across the samples obtained by the  $\mu$ -FTIR. The insets show maps of the uncompensated boron content in the samples with the locations of the fabricated diode structures.

## Results

Transmission  $\mu$ -FTIR mapping reveals a highly non-uniform, sector-dependent distribution of uncompensated boron concentration  $[N_a - N_d]$  across the substrate, where the {111} growth sectors exhibit the highest doping levels (up to  $\sim 10^{19}$   $\text{cm}^{-3}$ ) compared to the significantly lower boron incorporation ( $\sim 10^{17}$ - $10^{18}$   $\text{cm}^{-3}$ ) observed in the {001} and {113} sectors (Fig.3).

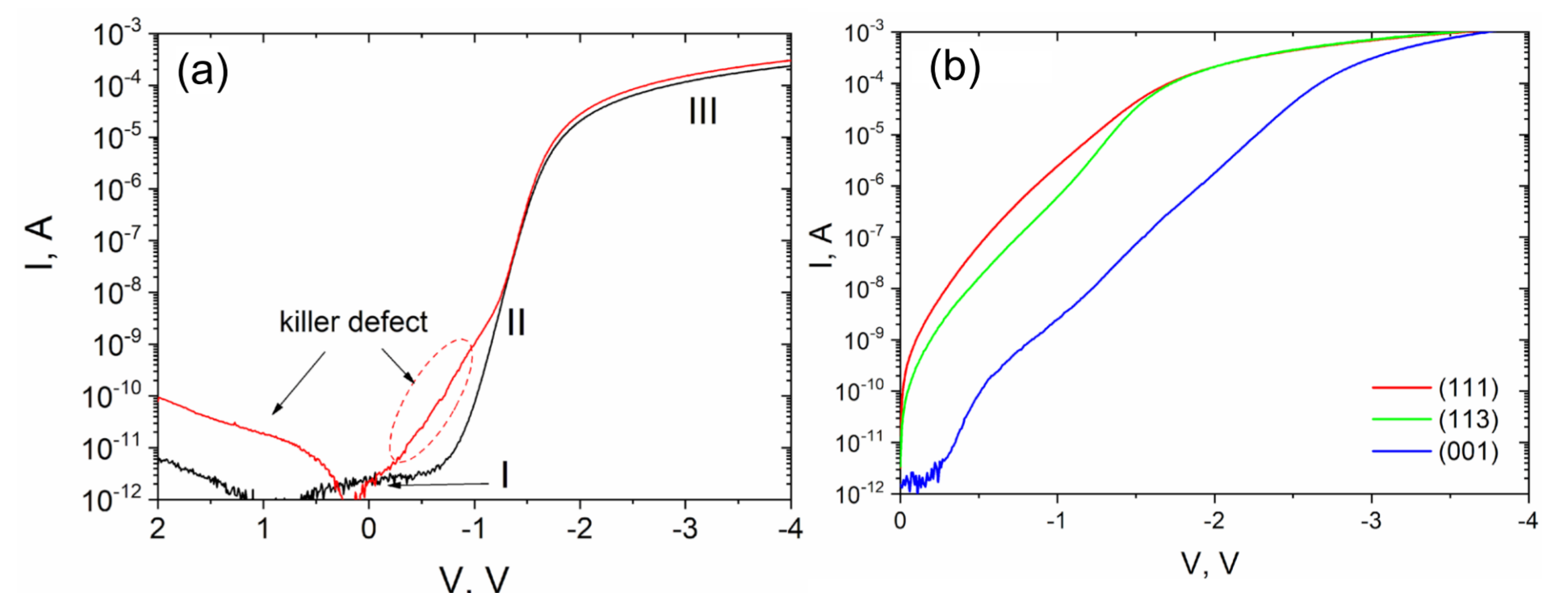


**Fig.4.** Current-voltage characteristics of an Au/Pt/Ni/diamond Schottky diode (a) on sample A: the black curve corresponds to a defect-free diode, while the red curve shows a diode containing a shunting (killer) defect. (b) on sample B for different sectors with varying dopant concentrations.

Electrical characterization of Ni/Pt/Au Schottky barriers demonstrates that this sectoral variation dictates two distinct transport regimes: diodes on low-doped {001} and {113} sectors exhibit excellent rectifying behavior with low leakage currents ( $I_{rev}$ ) limited only by discrete shunting defects, whereas in highly-doped {111} sectors, field-assisted tunneling causes a dramatic increase in reverse current and a transition toward ohmic-like behavior (Fig. 4).

The specific contact resistivity ( $\rho_c$ ) of Ti/Pt/Au ohmic structures is strongly modulated by both the base dopant concentration and sector affiliation, yielding systematically lower  $\rho_c$  values within the {001} and {113} sectors than in the {111} sectors for identical boron concentrations (Fig. 5). Since macroscopic shunting defects contribute negligibly to large-area ohmic transport, this distinct anisotropy is attributed to growth-sector-specific near-surface defect structures and unique solid-state reactions occurring at the metal-diamond interface during rapid thermal annealing.

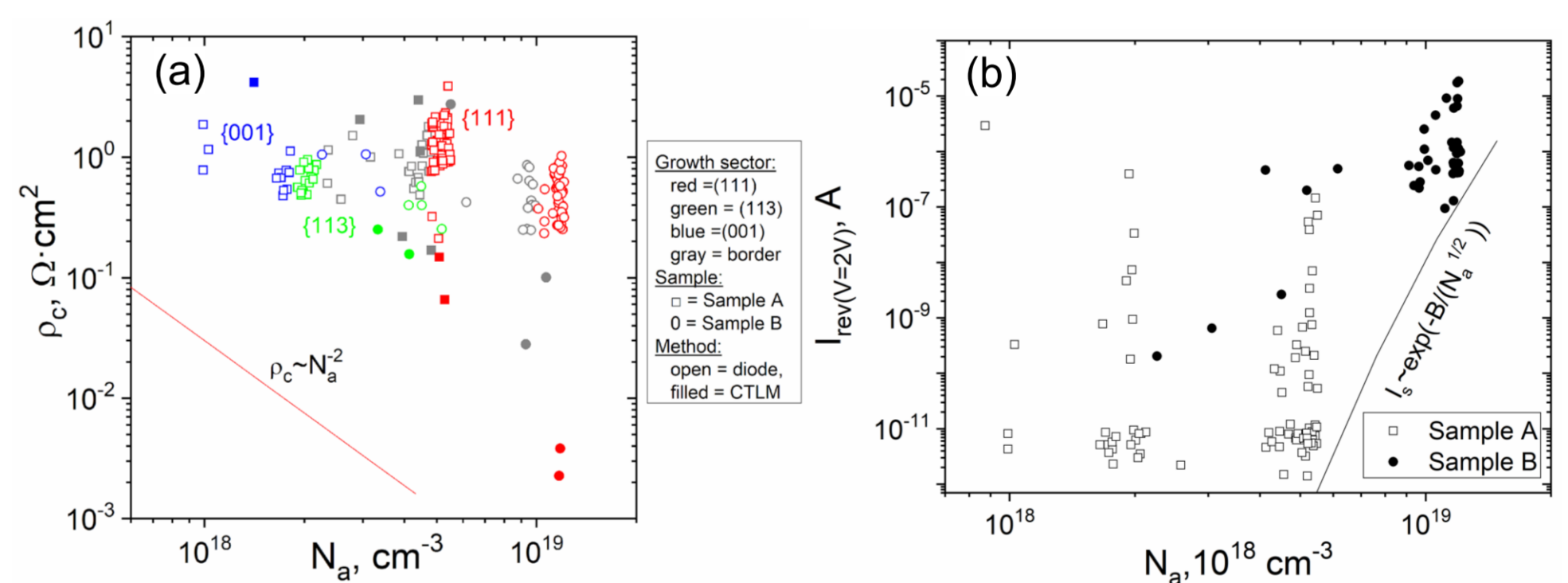


**Fig.5.** (a) Specific contact resistance as a function of uncompensated boron concentration for Ti/Pt/Au contacts fabricated on boron-doped HPHT diamond substrates. (b) Dependence of the current at a reverse bias of 2 V on the dopant concentration for both samples A and B.

**Table 1.** Quality yield of Schottky diodes by sectors (sample A).

Sector	(111)	(113)	(001)
Total diodes	40	13	15
Defect-free	24	7	10
Yield (%)	60	54	67

## Conclusions

In conclusion, this work demonstrates that the multi-sector growth structure of HPHT boron-doped diamond substrates strongly modulates the electrical characteristics of both Schottky barriers and ohmic contacts. Correlative micro-FTIR mapping and electrical measurements revealed that while localized, discrete shunting defects dictate early failures and leakage statistics in lower-doped {001} and {113} sectors, field-assisted tunneling becomes the dominant reverse transport mechanism in highly-doped {111} sectors. Furthermore, we established a clear growth-sector-dependent anisotropy in specific contact resistivity for Ti/Pt/Au ohmic contacts, where {001} and {113} faces systematically yield lower resistance compared to {111} faces for identical boron concentrations. These findings emphasize that achieving high-performance diamond electronics requires careful consideration of growth-sector boundaries and interface-specific defect chemistry during device design and substrate selection.

## Acknowledgements

The authors are grateful to the National Research Foundation of Ukraine for financial support in the framework of the project № 2020.02/0160 "Development of new carbon solvents compositions for diamond single crystals growth in the thermodynamic stability area with a controlled content of nitrogen and boron impurities in order to create conceptual electronic devices construction".